J. Fluid Mech. (1982), *vol.* 123, *pp.* 379–398
Printed in Great Britain

Strouhal numbers of rectangular cylinders

By ATSUSHI OKAJIMA

Research Institute for Applied Mechanics, Kyushu University,
Hakozaki, Higashi-ku, Fukuoka, 812, Japan

(Received 17 September 1981 and in revised form 18 March 1982)

Experiments on the vortex-shedding frequencies of various rectangular cylinders were conducted in a wind tunnel and in a water tank. The results show how Strouhal number varies with a width-to-height ratio of the cylinders in the range of Reynolds number between 70 and 2×10^4. There is found to exist a certain range of Reynolds number for the cylinders with the width-to-height ratios of 2 and 3 where flow pattern abruptly changes with a sudden discontinuity in Strouhal number. The changes in flow pattern corresponding to the discontinuity of Strouhal number have been confirmed by means of measurements of velocity distribution and flow visualization. These data are compared with those of other investigators. The experimental results have been found to show a good agreement with those of numerical calculations.

1. Introduction

Detailed information regarding flows around rectangular cylinders in a uniform flow is of special interest for the basic understanding of aerodynamics, and is of great importance in the study of aeroelastic instability.

Many works with good results have been reported in this field (e.g. Parkinson & Brooks 1961; Scruton 1963; Vickery 1966; Nakaguchi, Hashimoto & Muto 1968; Bearman & Trueman 1972; Bostock & Mair 1972; Novak 1972; Otsuki *et al.* 1974; Lee 1975; Nakamura & Mizota 1975). In particular, Nakaguchi *et al.* (1968) found that the width-to-height ratio of rectangular cylinder is one of the major contributing factors to the aerodynamic characteristics. Recently, Mizota & Okajima (1981*a*, *b*), using a tandem type of hot-wire probe, measured successfully flow patterns around various rectangular cylinders including a reversed flow region close to the cylinders, and confirmed that the changes of the flow patterns have close correlations with those of drag and lift forces and Strouhal numbers in the variation of the width-to-height ratio and the angle of incidence.

In a case of a sharp-edged body like a rectangular cylinder, where the separation points are fixed at the leading edges, the aerodynamic characteristics are said to be relatively insensitive to Reynolds number.

At extremely low Reynolds number, flow around a rectangular cylinder is known to separate at the trailing edges rather than the leading edges where the separation is indiscernible owing to immediate reattachment. With an increase of Reynolds number, the flow separation at the leading edges will develop, and the steady reattachment becomes impossible. On the other hand, the phenomenon of transition from laminar to turbulent flow, which occurs in flow near the cylinder at certain values of the Reynolds number, should be taken into consideration.

Consequently it is quite likely that there exists a certain range of Reynolds number where the flow characteristics, the Strouhal number in particular, of a rectangular

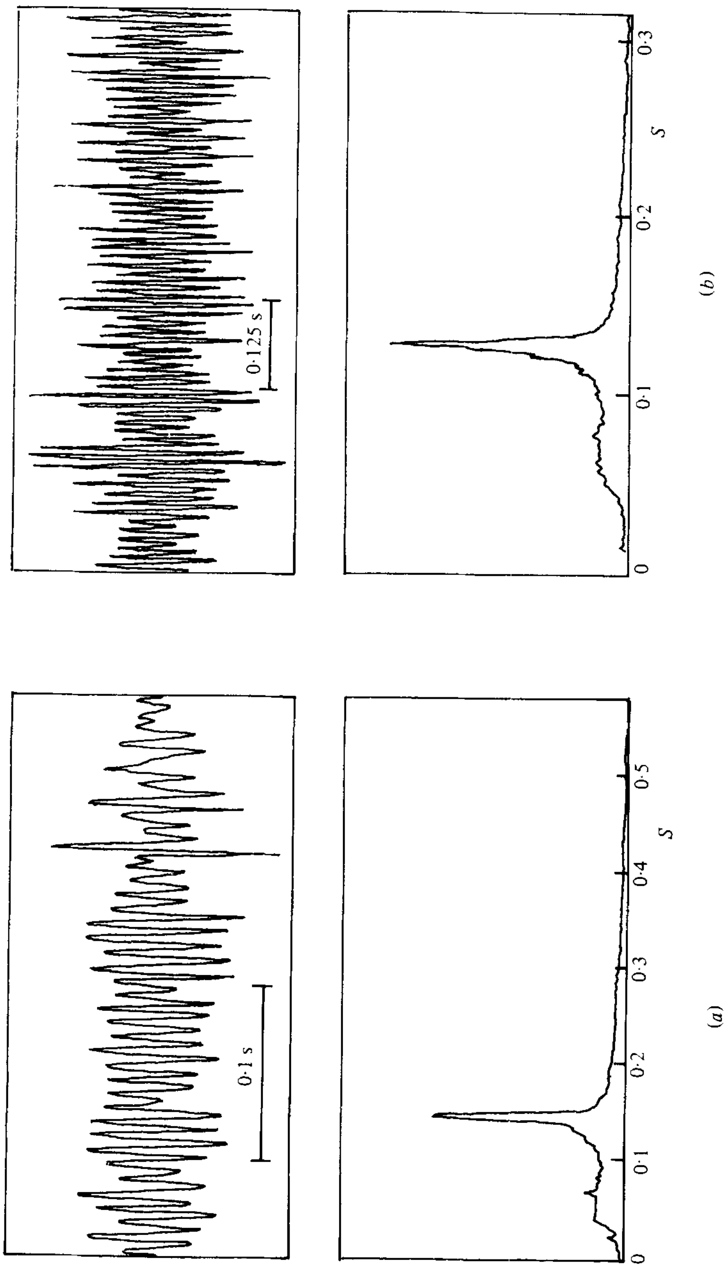

FIGURE 1. Signal traces and power spectra of fluctuating velocity in the wake for a square cylinder: (*a*) $R = 250$; (*b*) 2910.

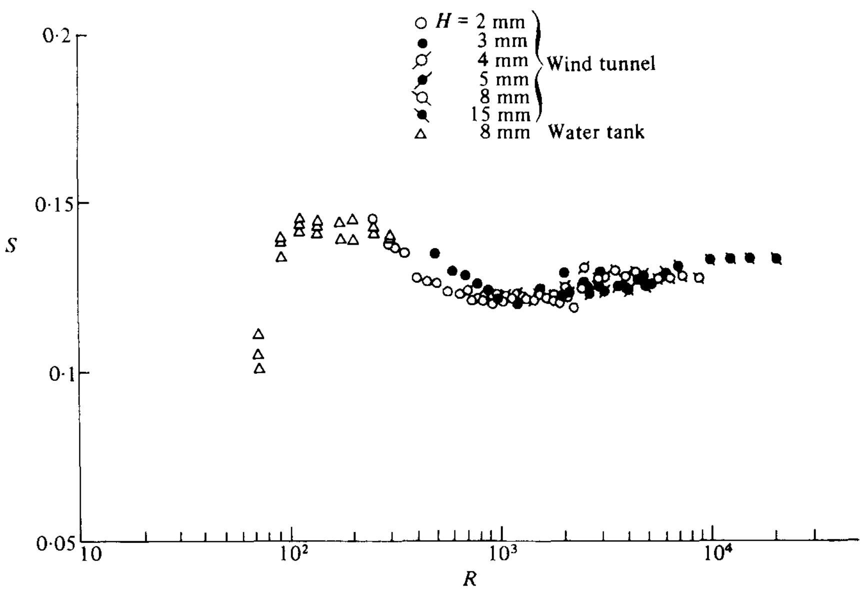

FIGURE 2. Variation of Strouhal number with Reynolds number for a square cylinder.

cylinder alter remarkably. The existing measurements, however, are valid only at high Reynolds number and there is a lack of information at relatively low Reynolds number.

The present study is therefore intended to determine the Strouhal number of various rectangular cylinders as a function of Reynolds number, and to examine the velocity distributions and flow patterns around the cylinders. The experiments, performed in either air or water, cover a relatively wide range of Reynolds number between 70 and 2×10^4, and the results have been confirmed by comparison with those of numerical calculations (Okajima & Sugitani, 1979), as well as those available in experimental works by other investigators.

2. Experimental apparatus

The present study requires a relatively wide range of Reynolds number. An open-jet small wind tunnel and a towing-type water tank are used for that purpose. Flow-visualization tests are conducted in a water tank.

2.1. *Wind tunnel*

Strouhal number and velocity distributions in the wake are measured in a small wind tunnel. The test section is 200 mm in height and 200 mm in width. The rectangular cylinder models are made of brass, with width-to-height ratios, B/H (B is a side length of the cylinder and H is its height) of 1, 2, 3 and 4, and the dimension H is 2–15 mm. Aspect ratios of the models are between 13·3 and 100. All models are very small, their corners being sharp and their surfaces as smooth as possible. Tested wind velocity U is in the range 1·5–20 m/s, so that the Reynolds number $R = UH/\nu$, where ν is the kinematic viscosity, varies between 200 and 2×10^4. The intensity of free-stream turbulence is less than 0·5 %. The frequencies f of vortex shedding generated by the various models are measured by a hot-wire probe placed in a position with

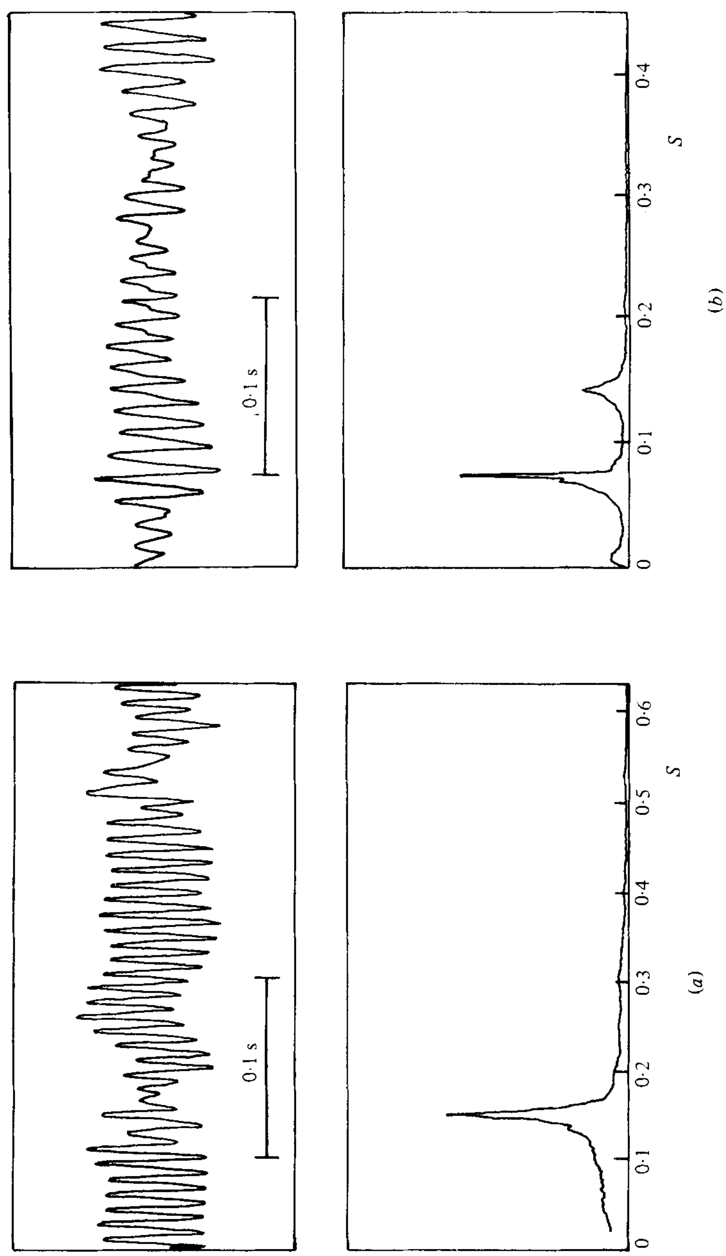
0·1 s
0
0·1
0·2
0·3
0·4
S
(b)
0·1 s
0
0·1
0·2
0·3
0·4
0·5
0·6
S
(a)

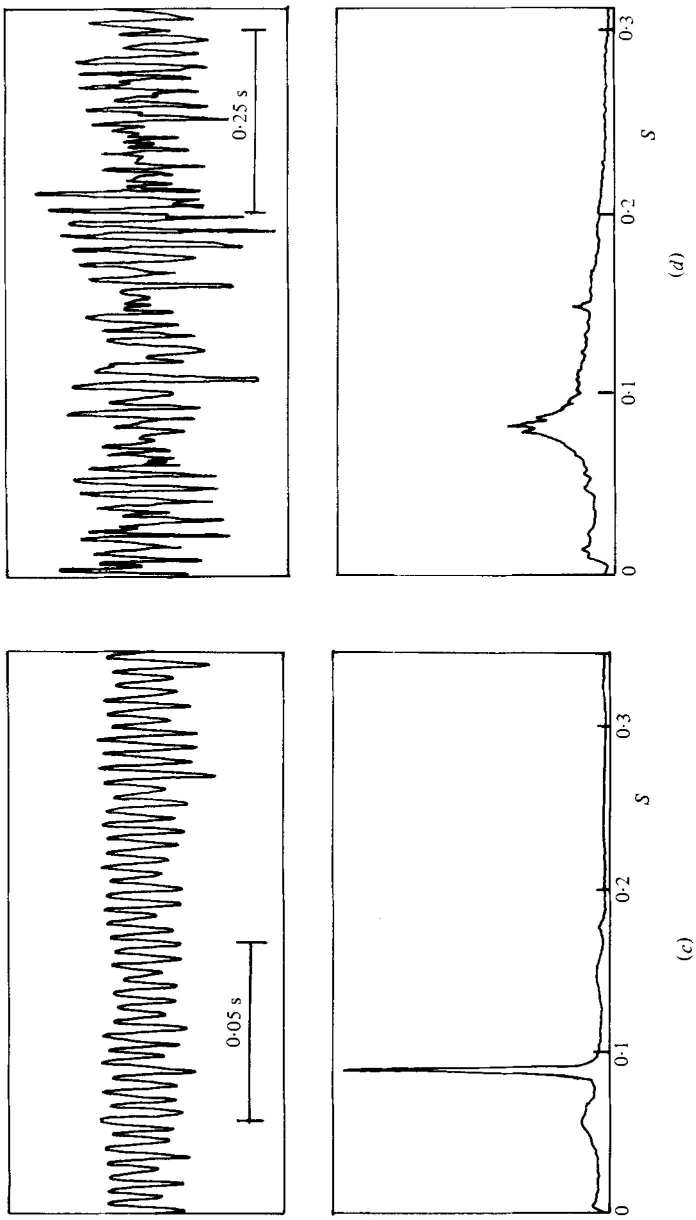

FIGURE 3. Signal traces and power spectra of fluctuating velocity in the wake for a rectangular cylinder with $B/H = 2$: (*a*) $R = 226$; (*b*) 500; (*c*) 1200; (*d*) 10200.

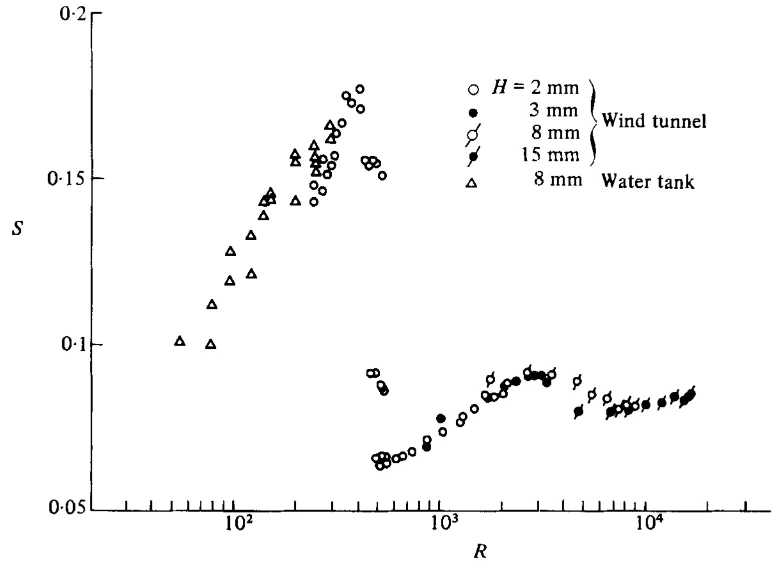

FIGURE 4. Variation of Strouhal number with Reynolds number for a rectangular cylinder with $B/H = 2$.

$x/H = 6{\cdot}0$–$11{\cdot}5$, $y/H = 4{\cdot}5$–$5{\cdot}0$ in the wake, and all the resulting data are analysed by a Fourier frequency analyser. Strouhal number is then defined by $S = fH/U$.

2.2. *Water tank*

Tests at values of the Reynolds number below about 300 are conducted in a water tank. The tank is 0·4 m wide by 6 m long, with a water depth of 0·4 m. A model is made of brass, with 300 mm span length, and the frequency of a wake is detected by a hot-wire probe devised to be efficient in water. In the experiments in the water tank, flow-visualization tests are carried out in addition, the aluminium-dust method and the electrolytic-precipitation method being employed at the same time. The aluminium method has the merit of enabling a direct comparison with the streamline plots of the numerical calculations, since the velocity vector defined by the aluminium particles must lie tangent to a streamline. In the electrolytic-precipitation method, white dye of a metallic compound is produced electrochemically only from the front surface of the cylinder, clearly showing streaklines of the flow separated around the model.

3. Experimental results

3.1. *Frequency of vortex shedding*

3.1.1. *A square-section cylinder.* Figure 1 shows typical examples of recorded signal traces and the power spectra of a fluctuating velocity in the wake of a square cylinder for increasing Reynolds number. It is evident that the wake velocity fluctuates in a fairly sinusoidal wave, which results in a single and sharp spectral peak at the predominant frequency. It indicates the onset of strong vortex shedding in the wake for all cases. Figure 2 summarizes the variation of Strouhal number with Reynolds number obtained in both air and water. Broadly speaking, Strouhal numbers of a square cylinder show slight and continuous change around a constant value in the wide range of Reynolds number between 10^2 and $2{\cdot}0 \times 10^4$. The value of Strouhal number near high values of Reynolds number between 10^4 and 2×10^4 is 0·13, in close agreement with the most widely accepted data in the literature (e.g. Nakaguchi *et al.* 1968; Otsuki *et al.* 1974).

3.1.2. *A rectangular cylinder with* $B/H = 2$. Figures 3 and 4 exhibit respectively the power spectra and Strouhal numbers of the wake behind a rectangular cylinder with $B/H = 2$, for increasing Reynolds number.

In the Reynolds-number range below 400, there is just a single sharp peak in the power spectrum, as shown in figure 3(*a*) ($R = 226$). At $R = 500$ an interesting phenomenon of two predominant frequencies with sharp peaks appears as in figure 3(*b*). The lower frequency of the two peaks is just a subharmonic of the higher one. The appearance of the subharmonic component corresponds to the signal traces alternately changing in amplitude every cycle as shown in this figure.

With further increase of Reynolds number, the lower-frequency component is seen to grow, accompanied by a disappearance of the higher-frequency component in power spectra, as shown in figure 3(*c*) ($R = 1200$). And at higher Reynolds number, e.g. $R = 10200$ (figure 3*d*), the irregularity begins to appear in the signal waves and the spectral peak becomes gradually broader, its periodicity being persistent.

Figure 4 is a plot of Strouhal number versus Reynolds number. The above-mentioned discontinuity in the Strouhal-number curve becomes clearly discernible near $R = 500$. Namely, at Reynolds numbers below this value, Strouhal number increases with Reynolds number, reaching the value of 0·18. Then a striking feature of a sharp decrease in the Strouhal-number curve follows abruptly beyond that Reynolds number. This phenomenon is clearly related to sudden changes in the flow patterns, which will be described later. For $R > 600$, the lower-frequency component becomes dominant, and a gradual increase is seen in the Strouhal number. When $R > 5 \times 10^3$, Strouhal number remains nearly constant at 0·08–0·09, being consistent with the data of Nakaguchi *et al.* (1968) and Otsuki *et al.* (1974).

3.1.3. *Rectangular cylinders with* $B/H = 3$ *and* 4. Figures 5 and 6 show the power spectra and Strouhal numbers of a fluctuating velocity in the wake for a rectangular cylinder with $B/H = 3$.

In this case, the Reynolds-number region in which the spectrum has more than one peak associated with complicated changes of the flow patterns becomes rather high and wide, viz from 10^3 to 3×10^3. At Reynolds numbers below that, the wake velocity oscillates sinusoidally, resulting in a single sharp peak of the power spectrum, as shown in figure 5(*a*) ($R = 500$).

At $R = 1000$ (figure 5*b*) there can be found a small peak in the lower-frequency range in addition to the dominant peak, $S = 0{\cdot}16$. When the Reynolds number reaches 1220, two different kinds of signal wave are noticed, as shown in figure 5(*c*). They are quite different in amplitude and frequency, and appear alternately with a rather long period. The regular waves with small amplitude and high frequency, $S = 0{\cdot}16$ of figure 5(*e*) (here referred to as 'mode I') are intermittently replaced by the other waves of figure 5(*d*) with larger amplitude and lower frequency. The latter waves are referred to as 'mode II'. The mode II waves are rather irregular in shape and are further resolved into two kinds of dominant peak at Strouhal numbers of 0·06 and 0·12 in the power spectrum of figure 5(*d*). Therefore in this region three distinct values of Strouhal number can be plotted at one Reynolds number, as shown in figure 6.

A gradual increase of Reynolds number in this region leads to the disappearance of the highest-frequency component due to mode I, accompanied by the development

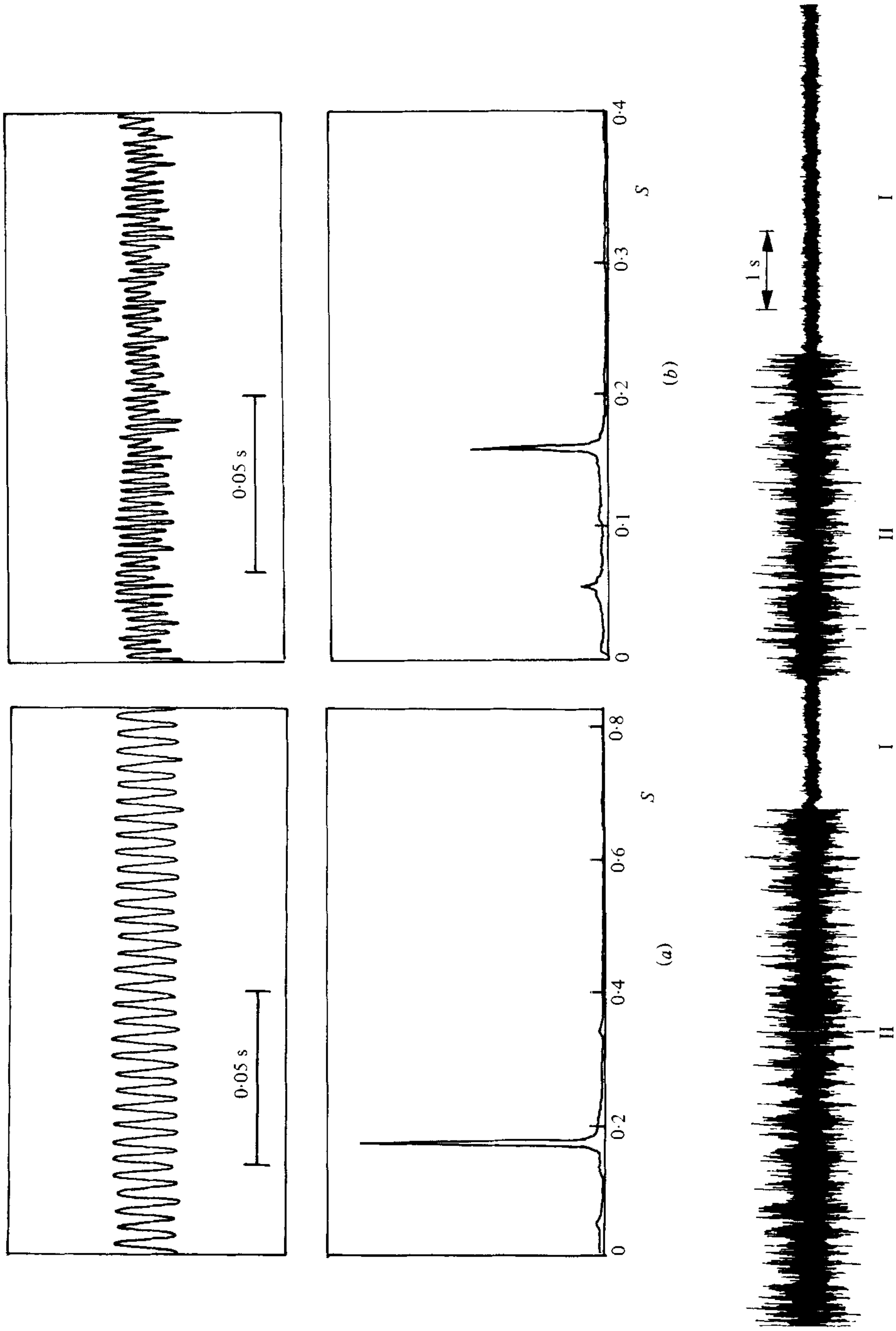
0·05 s
0·05 s
0
0·1
0·2
0·3
0·4
S
(b)
0
0·2
0·4
0·6
0·8
S
(a)
1 s
I
II
I
II
(c)

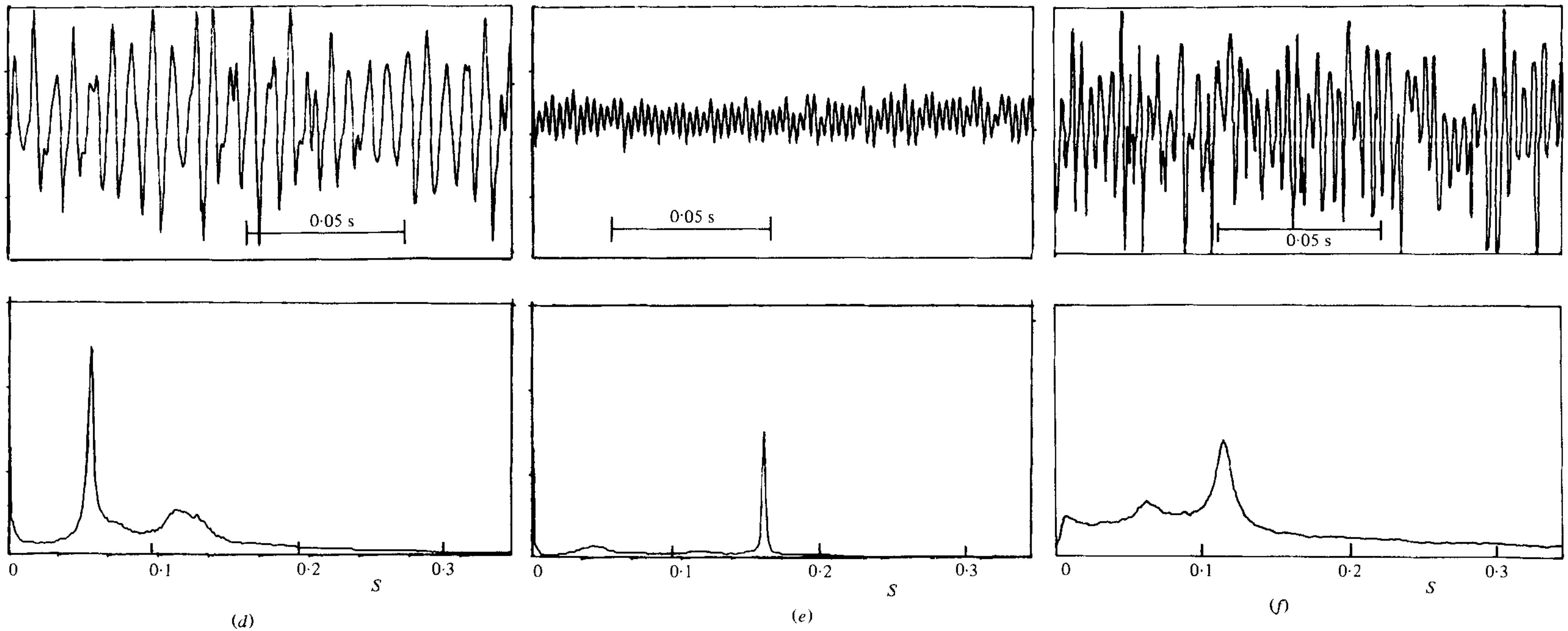

FIGURE 5. Signal traces and power spectra of fluctuating velocity in the wake for a rectangular cylinder with $B/H = 3$: (a) $R = 500$; (b) 1000; (c) 1220; (d) 1220; (e) 1220; (f) 1920.

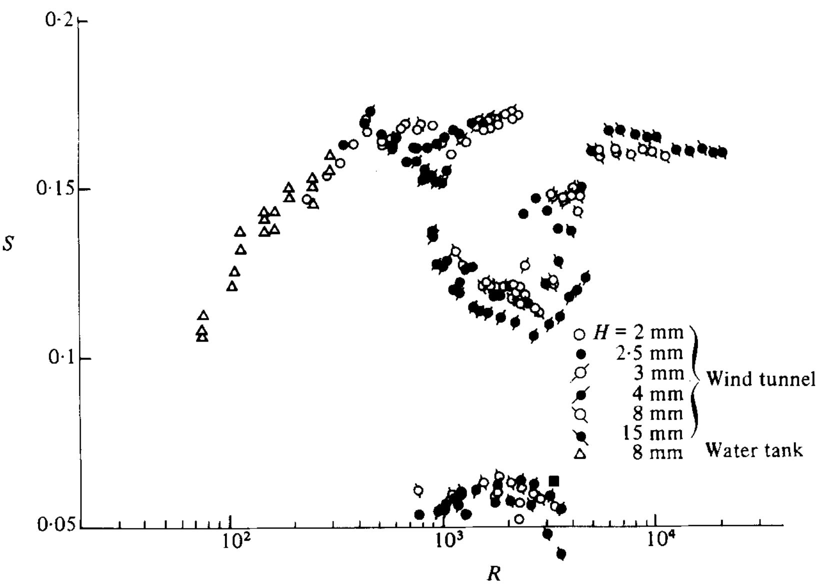

FIGURE 6. Variation of Strouhal number with Reynolds number for a rectangular cylinder with $B/H = 3$.

of the two frequency components due to mode II; the decay of the lower component of mode II follows. Thus at high Reynolds numbers only the higher-frequency component of mode II remains dominant, as illustrated in figure 5 (f), and the value of Strouhal number approaches 0·16–0·17, which is the same as that of mode I as shown in figure 6. The appearance of these three peaks, however, has a degree of uncertainty; that is, the value of Reynolds number at which the component of the highest or the lowest frequency disappears is different according to the size of the models or the experimental method of changing the wind velocity.

Finally the results of a long model with $B/H = 4$ are presented in figure 7. As is obvious from this figure, Strouhal number is almost independent of Reynolds number. All recorded signal traces are regular enough to yield a single sharp peak in power spectra.

3.2. *Velocity distribution of the wake*

In order to confirm the phenomenon of the discontinuity in the Strouhal-number curves, the velocity distributions of the wake are measured for some cylinders. Figure 8 presents the wake profiles at three different values of R, 300, 900 and 1770, for a rectangular cylinder with $B/H = 2$. At $R = 300$, which is lower than the critical value of about 500, the wake width is narrow and two peaks of the fluctuating component $(\overline{u'^2})^{\frac{1}{2}}/U$ are near the centre of the mean-velocity distribution. In the cases of higher $R = 900$ and 1770, however, the wakes are fairly wide and the fluctuating components become diffused. The sudden decrease in the Strouhal-number curve of figure 4 is apparently due to this widening of the wake.

Next, figures 9 (a, b) show the wake profiles for the cylinder with $B/H = 3$. The velocity distributions at $R = 1100$ of figure 9 (a), corresponding to the critical region, are distinct and interesting. The solid and the dotted lines in this figure are the plots of the alternate appearance of two kinds of flow patterns obtained from

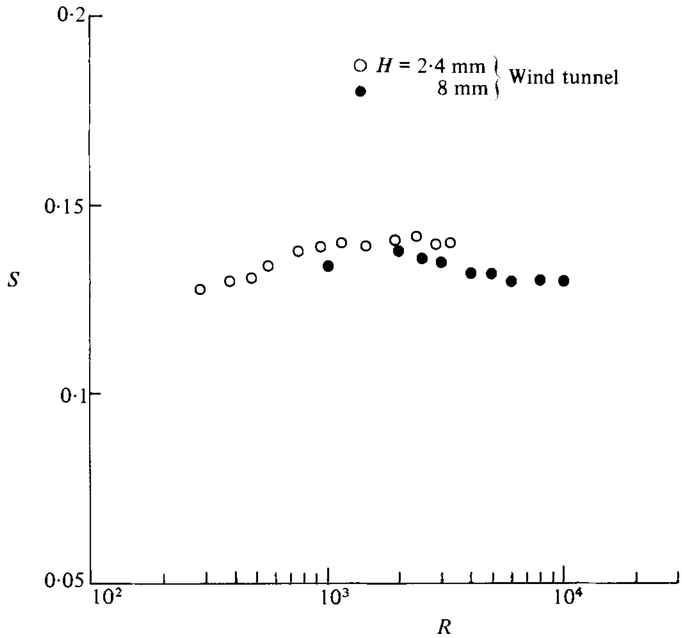

FIGURE 7. Variation of Strouhal number with Reynolds number for a rectangular cylinder with $B/H = 4$.

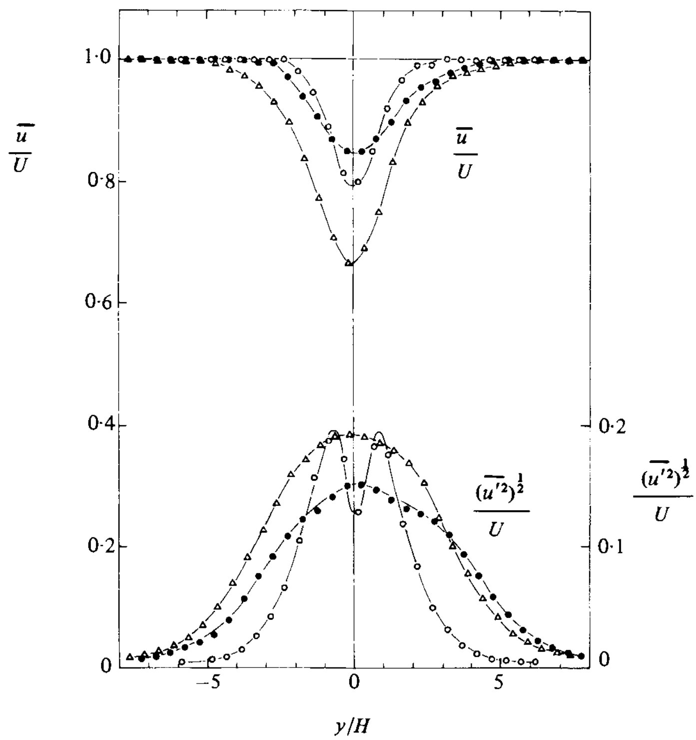

FIGURE 8. Velocity distributions in the wake for a rectangular cylinder with $B/H = 2$: ○——○, $R = 300$; ●——●, 900; △——△, 1770. (The position of a hot wire is $x = 11{\cdot}5H$ from the rear of a cylinder.)

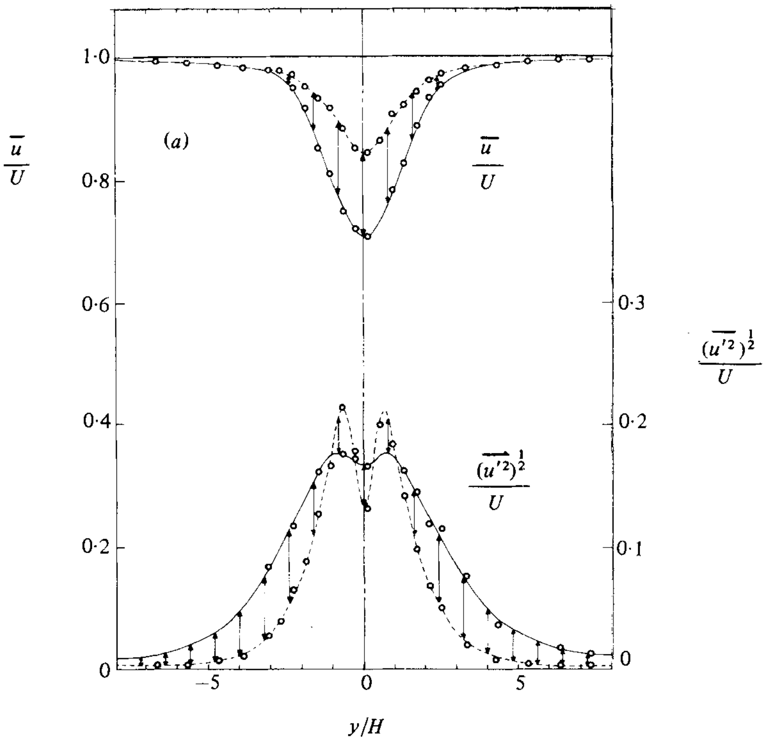

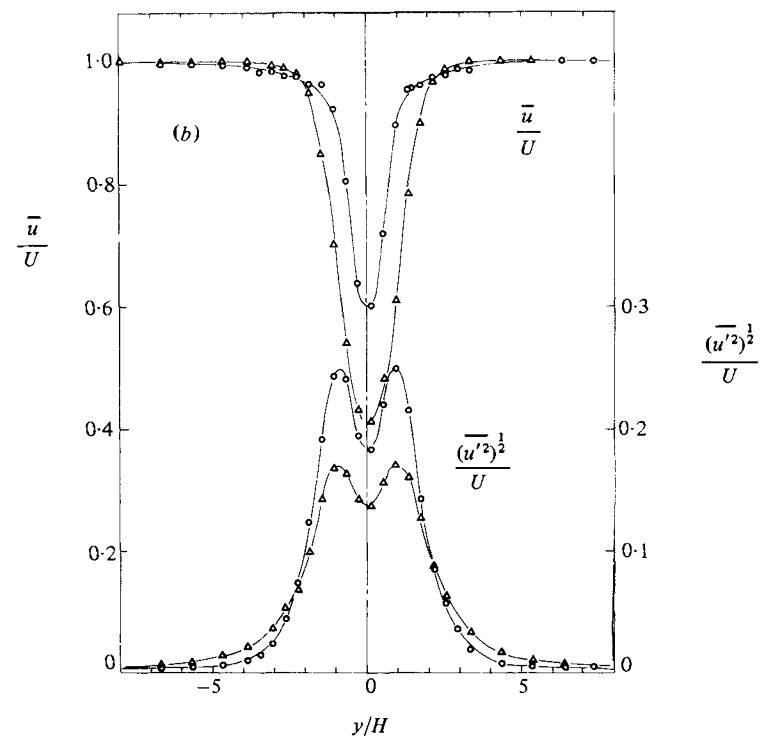

FIGURE 9. Velocity distributions in the wake for a rectangular cylinder with $B/H = 3$. (a) $R = 1100$: ○---○, mode I; ○——○, mode II. (b) ○——○. $R = 500$; △——△, 2500. (The position of a hot wire is $x = 6{\cdot}0\,H$ from the rear of a cylinder.)

observation over a long period. The dotted profile with the narrower wake width corresponds to the mode I, which implies that, after separating from the leading edges, the flow reattaches on the side surfaces and that vortex shedding with high frequency 0·16 results from final separation at the trailing edges. Mode II is shown by the other profile of the wide wake width, which indicates that reattachment becomes impossible. It can be clearly and easily observed during the experiments that mode I alternates intermittently with mode II.

Figure 9(*b*) exhibits the wake profiles at $R = 500$ and 2500, both of which values are outside the above-mentioned region. At low $R = 500$, the amplitude of the fluctuating component is fairly large, with 25 % of the uniform velocity, and the width of the wake is narrow and almost the same as the height of the model. At $R = 2500$, the minimum value of the mean-velocity distribution reaches 0·4 of the uniform velocity and the wake becomes wide, being about 1·4 times the height of the model.

4. Discussion

4.1. *Comparison between experimental results and calculated values*

When Reynolds numbers are as low as 150, 250 and 600, numerical calculations of flows around rectangular cylinders have been carried out by the author (Okajima & Sugitani 1979). Figures 10(*a*, *b*) and 11 present flow patterns around the cylinders with $B/H = 1$ and 2 respectively. These calculations are limited to laminar flow. In all cases excellent agreement can be observed between the experiments and the calculations at two different instances of vortex sheddings from the lower and the upper surfaces of the cylinder.

For the square cylinder in figures 10(*a*, *b*), flow separation is observed at the leading edges, followed by rolling up behind the cylinder. Daiguji & Kobayashi (1981) recently calculated flows around a square cylinder and presented the flow patterns at $R = 80$, where flow separates just at the trailing edges without a sign of the separation at the leading edges. However, in the present results of $R = 150$ and 250, flow is seen to detach itself on either the upper or the lower surface.

For the rectangular cylinder with $B/H = 2$, it is evident from figure 11 that at $R = 250$ the separated flow goes along the surfaces and always reattaches on either the upper or the lower surface during a period of the vortex shedding into the wake.

Next, the time variation of the calculated flow patterns for $B/H = 2$ at $R = 600$ is given in figure 12. This Reynolds number is known to be in the range of the critical region. The figure covers twice the period of the vortex shedding from time 48·0 to 69·0, and the flow patterns experience rather complicated changes. Three patterns at times 48·0, 58·5 and 69·0 in figure 12 each show the shedding of an eddy from the upper surface – these eddies are of similar shape. From detailed comparison among these patterns, the one at time 48·0 is identical with that at time 69·0.† However, some differences can be observed between those at time 48·0 (or 69·0) and 58·5.‡

Consequently, a series of these changes in flow patterns makes it clear that the vortex streets are shed behind the cylinder with two different frequencies: 1/10·5 and its subharmonic frequency 1/21·0. The calculated values of the frequency are slightly lower than the experimental ones. The discrepancy seems to be attributable to numerical errors. However, it is remarkable and important that the same phenomena that are found in experiments can be simulated by the numerical calculations.

† The patterns at times 27·0, 48·0 and 69·0, where the instantaneous reattachment occurs near the upper trailing edge, are the same in shape.

‡ The patterns at times 37·5 and 58·5 are also identical. Their flows detach themselves fully both on the upper and the lower surfaces.

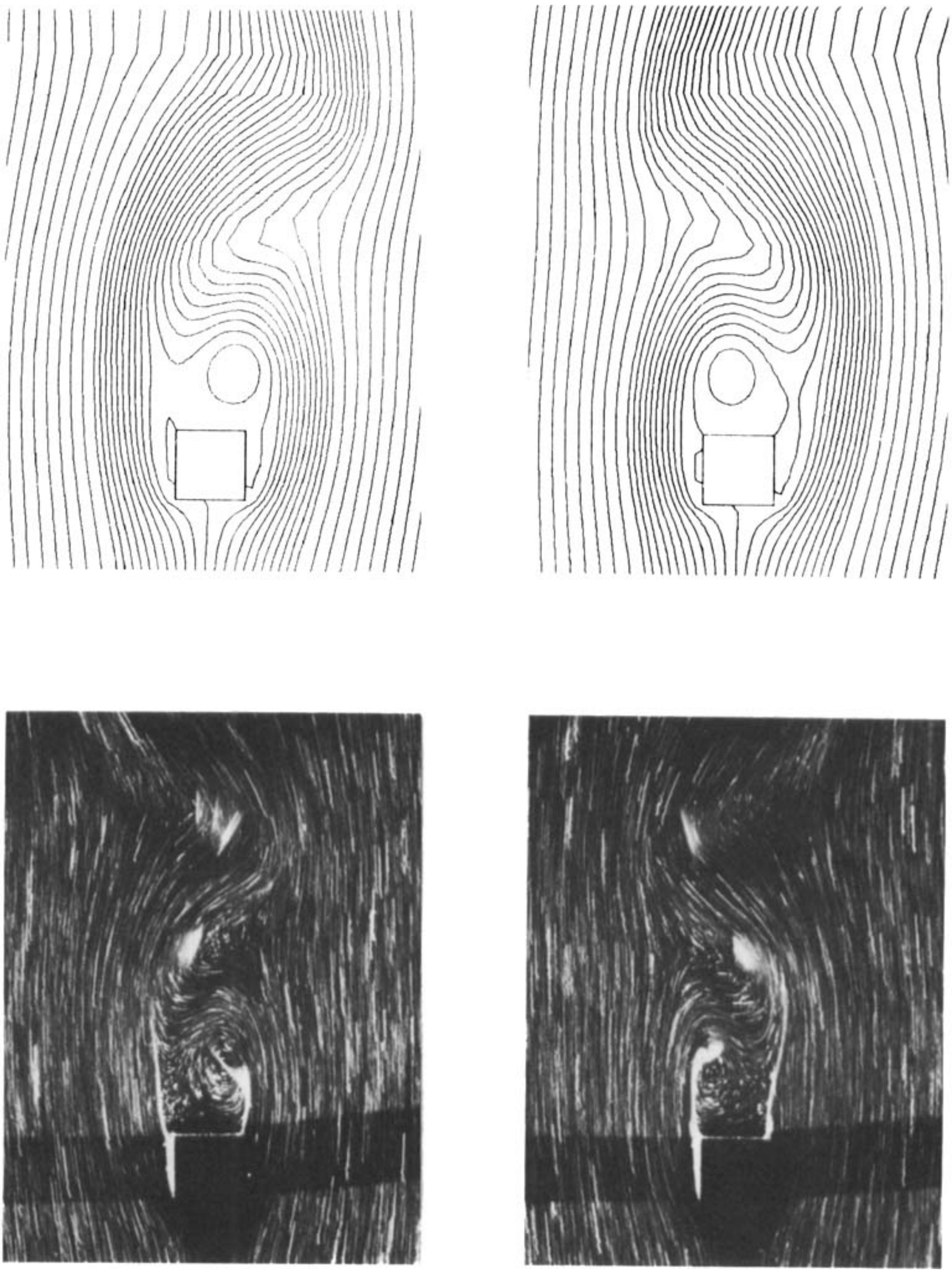

(a)

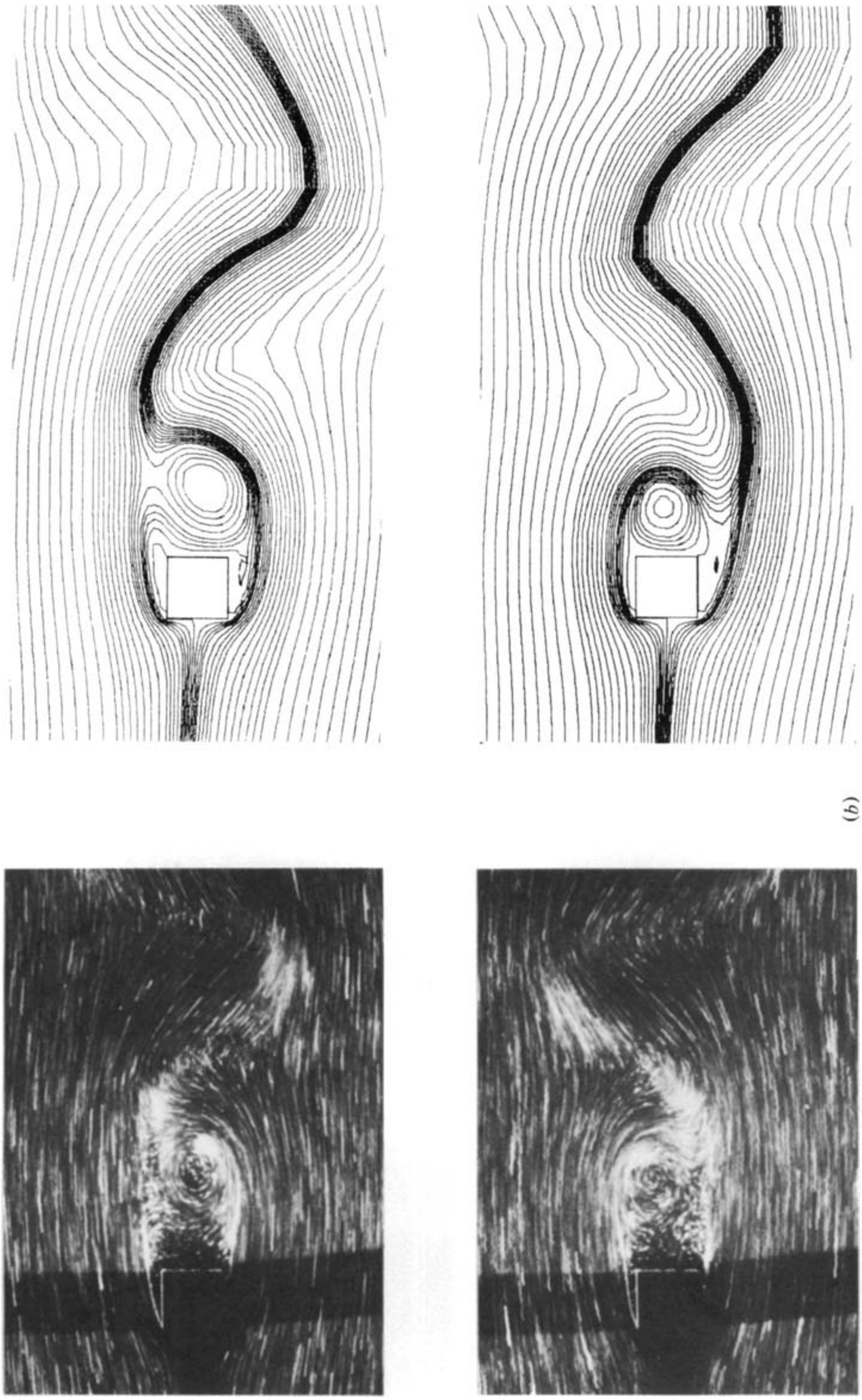

FIGURE 10. A comparison between visualized flow patterns and theoretical predictions for a square cylinder: (a) $R = 150$; (b) 250.

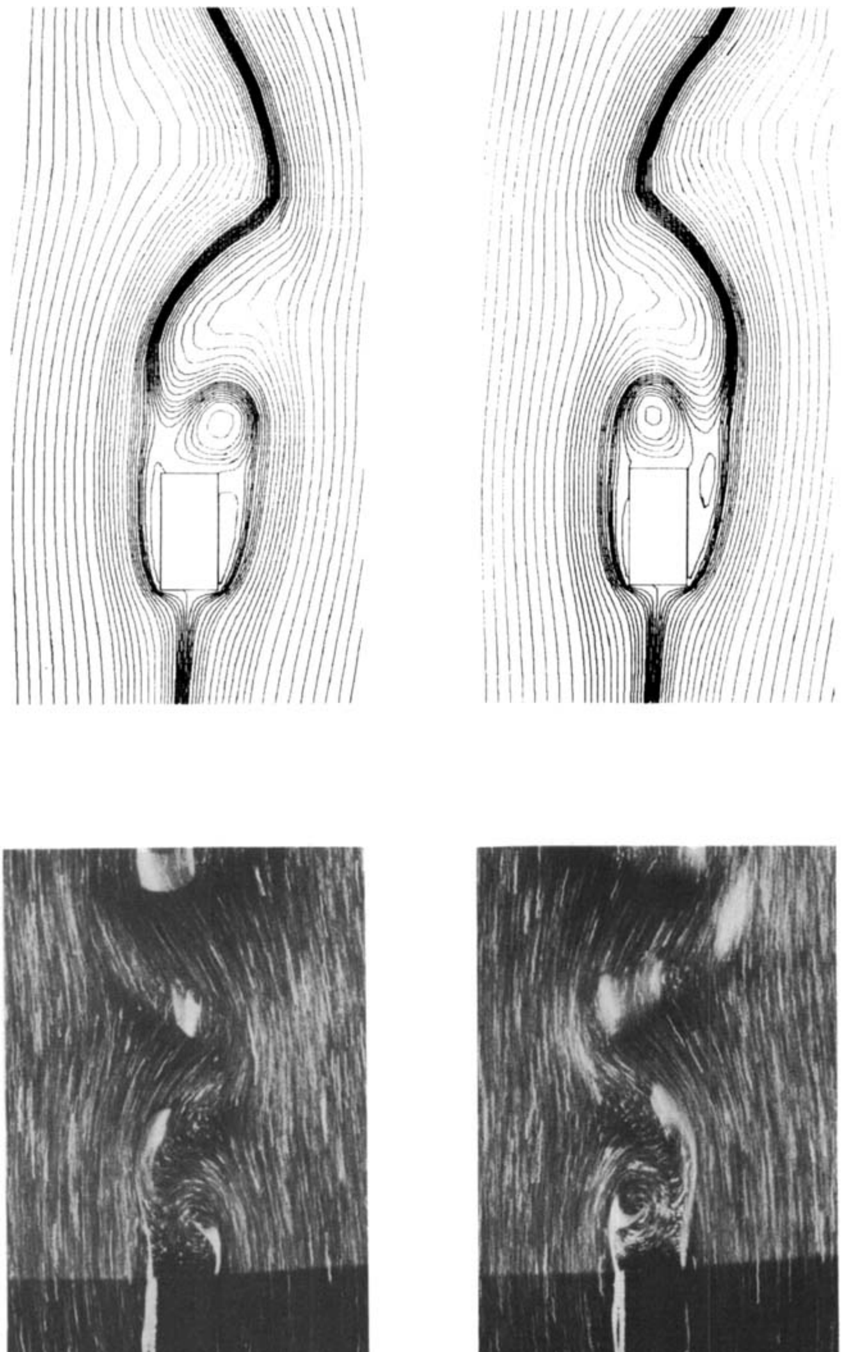

FIGURE 11. A comparison between visualized flow patterns and theoretical predictions for a rectangular cylinder with $B/H = 2$ at $R = 250$.

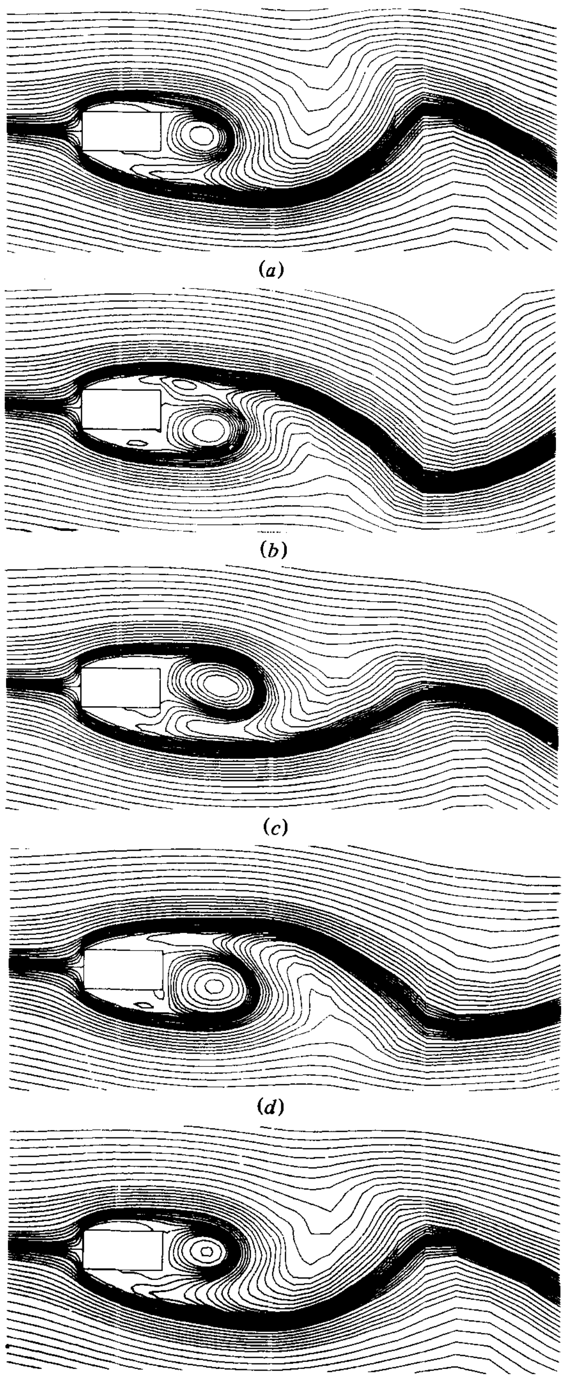

FIGURE 12. Time variation of calculated flow patterns around a rectangular cylinder with $B/H = 2$ at $R = 600$: (*a*) $t = 48{\cdot}0$; (*b*) 53·25; (*c*) 58·5; (*d*) 63·75; (*e*) 69·0.

Unfortunately, it is at present impossible to carry out the simulation for the case with $B/H = 3$ and $R \approx 10^3$, since the theory is based upon a laminar-flow condition.

4.2. *Flow pattern changes with Reynolds number*

The region of Reynolds number where the discontinuity occurs in the Strouhal-number curve is strongly dependent on the B/H ratio of rectangular cylinders.

In the experiments with a square cylinder, such a region has not appeared. Recently Tomonari (personal communication), using a smoke-visualization technique, measured the distance of the transition point from laminar to turbulent flow for this cylinder at Reynolds numbers between 10^3 and 10^4. He confirmed that at $R \approx 10^3$ the transition occurs downstream of the trailing edges, and that an increase in R moves this point upstream. This movement of the transition point, however, does not cause a great change, such as a reattachment, for this cylinder.

When $B/H \gtrsim 2$, there appears distinctly a region of Reynolds number where the Strouhal number suddenly changes. The variation of the flow pattern thus depends entirely upon Reynolds number.† At extremely low Reynolds numbers, of course, there is a steady reattachment just behind the leading edges, and flow finally separates at the trailing edges. At moderate Reynolds numbers, flow separation at the leading edges is developed and the separated flows cannot detach themselves fully from the cylinder but reattach on either the upper or the lower surface during a period of vortex shedding; that is, the steady reattachment cannot be formed as shown in figure 11. Further increase of Reynolds number makes the separated flows detach themselves suddenly from the surfaces, which results in a widening of the wake, accompanied by the discontinuous change of Strouhal number, as shown in figures 8 and 9. Roshko (1954) has shown that the shedding frequency is related to the width of the wake, the relation being roughly inverse. Then a sudden widening of the wake due to flow detachment requires a reduction in Strouhal number.

The critical range of Reynolds number is at approximately 500 for the cylinder with $B/H = 2$, and it is delayed until about 10^3–3×10^3 for that with $B/H = 3$. It is inferred that, the bigger is B/H, the higher is the critical value, since the increase in the length of after-body of the cylinder tends to prevent the separated flows from expanding and to keep themselves attached to the side surfaces.

However, the drastic change in Strouhal number does not appear for the cylinder with too-large side ratio of 4, where the flow separated at the leading edges remains reattached to the upper and the lower surfaces. It should be further noted that the positions of this reattachment move on the side surfaces. Recently Mizota & Okajima (1981*b*) confirmed from measurements of the flow pattern around such cylinders at $R = 4{\cdot}28 \times 10^4$ that, although the reattachment is certainly observed in the time-averaged flow pattern, its reattachment point is never stationary, and is instantaneously swept away downstream.

Here the strong effects of transition from laminar to turbulent flow on the change of Strouhal number must be taken into consideration. In the case of $B/H = 2$, the flow near the cylinder at $R \approx 500$ is scarcely turbulent. Therefore, even if the flow is laminar, the phenomenon of a sudden decrease in the Strouhal-number curve might occur, as shown by the numerical calculations. A gradual increase of Strouhal number

† Free-stream turbulence is also one of the major contributing factors to the variation of flow pattern. The present level of turbulence is about 0·5 %, but it was impossible to improve the wind tunnel, so the results presented are for this turbulence level and may involve its effects. The addition of free-stream turbulence would have an influence upon the reattachment and the detachment of flow.

is followed in the range of Reynolds number from 600 to 3×10^3 in figure 4, since the transition occurs therein, resulting in a decreased width of the free shear layer and wake, subjected to the increasing effects of Reynolds stresses and turbulent entrainment.

In the experiment on the cylinder with $B/H = 3$, however, two different modes appear alternately and intermittently with a long period in the region of Reynolds number from 10^3 to 3×10^3. With increasing Reynolds number within this range, the flow pattern with high frequency, i.e. mode I, begins to disappear, and mode II with two kinds of low frequency grows up and persists. The mode I flow reattaches on the side surfaces and a final separation occurs at the trailing edges. At Reynolds numbers from 10^3 to 3×10^3, those two peaks can be found in the spectrum of the surviving mode II, which indicates a mixture of two different flow patterns, the detached and the reattached. Beyond a Reynolds number of about 8×10^3, the value of the Strouhal number approaches that of mode I, $S = 0{\cdot}16$–$0{\cdot}17$, since the effects of turbulence make the reattached flow predominate.

It is well known that the critical value of B/H where the Strouhal number suddenly increases is nearly constant, i.e. 2·8 at high Reynolds number, and the increase of Strouhal number is due to the change of flow pattern from the detached to the reattached flow. Otsuki *et al.* (1974) report that two different Strouhal numbers appear between $B/H = 2{\cdot}0$ and 2·8 near the critical value at Reynolds numbers from $0{\cdot}2 \times 10^5$ to $3{\cdot}3 \times 10^5$. It should be noticed that $B/H = 3$ is in the neighbourhood of this critical value. At high Reynolds number, the separated flows reattach on the cylinder having a higher-than-critical value of B/H, owing to the effects of the Reynolds stresses and turbulent entrainment. When the Reynolds number is not so large, say 10^3, however, it tends to be difficult to keep the flow that is separated at the leading edges from being reattached on the side surfaces, even for a cylinder with $B/H = 3$. The Reynolds number being decreased, the region of the B/H ratio where two peaks appear in spectra is shifted from the values of 2·0–2·8 of Otsuki *et al.* (1974) to the larger value, i.e. 3·0. The critical value of B/H should be considered to be a function of Reynolds numbers.

5. Conclusion

Strouhal numbers of rectangular cylinders have been determined as a function of Reynolds number and the B/H ratio of the cylinder. The range of Reynolds number under investigation is between 70 and 2×10^4 and the B/H ratio varies from 1 to 4.

For the cylinders with $B/H = 2$ and 3 there is found to be a certain range of Reynolds number where the abrupt change of flow pattern occurs with a sudden discontinuity in the Strouhal-number curves. For R below this region, the flow separated at the leading edges reattaches on either the upper or the lower surface during a period of vortex shedding while, for R beyond it, the flow fully detaches itself from the cylinder. For $B/H = 3$, however, the separated flow tends to reattach on the cylinder owing to the increasing effects of the Reynolds stresses and turbulent entrainment at high Reynolds number. This change has been confirmed by the measurements of velocity distribution and flow visualization and by the numerical calculations.

The critical value of Reynolds number is seen to be strongly dependent upon the B/H ratio of the cylinder. The present results, however, are limited to the case where the turbulence intensity of the free stream is about 0·5%. The critical value of Reynolds number should be considered to be under the influence of the turbulence of free stream.

The author wishes to express his gratitude to Dr D. S. Whitehead and his colleagues at Cambridge University for helpful comments and a critical reading of the manuscript, and is indebted to Prof Y. Nakamura of the Research Institute for Applied Mechanics, Kyushu University, for his invaluable advice and to Mr K. Sugitani for his assistance.

REFERENCES

BEARMAN, P. W. & TRUEMAN, D. M. 1972 An investigation of the flow around rectangular cylinders. *Aero. Q.* **23**, 229–237.

BOSTOCK, B. R. & MAIR, W. A. 1972 Pressure distributions and forces on rectangular and D-shaped cylinders. *Aero. Q.* **23**, 1–6.

DAIGUJI, H. & KOBAYASHI, S. 1981 Numerical solution for the time-dependent two-dimensional viscous flows past obstacle. 2nd report: A stationary obstacle in a uniform flow. *Trans. Japan Soc. Mech. Engrs* B **47**, 9–15 (in Japanese).

LEE, B. E. 1975 The effect of turbulence on the surface pressure field of a square prism. *J. Fluid Mech.* **69**, 263–282.

MIZOTA, T. & OKAJIMA, A. 1981*a* Experimental studies of mean flow around rectangular prisms. *Proc. Japan Soc. Civ. Engrs* **312**, 39–47 (in Japanese).

MIZOTA, T. & OKAJIMA, A. 1981*b* Experimental studies of unsteady flow around rectangular prisms. *Proc. Japan Soc. Civil Engrs* **312**, 49–57 (in Japanese).

NAKAGUCHI, H., HASHIMOTO, K. & MUTO, S. 1968 An experimental study of aerodynamic drag of rectangular cylinders. *J. Japan Soc. Aero. Space Sci.* **16**, 1–5 (in Japanese).

NAKAMURA, Y & MIZOTA, T. 1975 Unsteady lifts and wakes of oscillating rectangular prisms. *Proc. A.S.C.E.: J. Engng Mech. Div.* **101** (EM6), 855–871.

NOVAK, M. 1972 Galloping oscillations of prismatic structures. *Proc. A.S.C.E.: J. Engng Mech. Div.* **98** (EM1), 27–45.

OKAJIMA, A. & SUGITANI, K. 1979 Flows around rectangular cylinders. Numerical calculations and experiments, part 2. *Bull Res. Inst. Appl. Mech., Kyushu Univ.* **50**, 67–80 (in Japanese).

OTSUKI, Y., WASHIZU, K., TOMIZAWA, H. & OYA, A. 1974 A note on the aeroelastic instability of a prismatic bar with square section. *J. Sound Vib.* **34**, 233–248.

PARKINSON, G. V. & BROOKS, N. P. H. 1961 On the aeroelastic instability of bluff cylinders. *Trans. A.S.M.E.* E: *J. Appl. Mech.* **28**, 252–258.

ROSHKO, A. 1954 On the drag and shedding frequency of two-dimensional bluff bodies. *NACA Tech. Note* no. 3169.

SCRUTON, C. 1963 The wind-excited oscillations of stacks, towers and masts. In *Proc. N.P.L. Symp.* no. 16, *Wind effects on buildings and structures.* H.M.S.O. (London) paper no. 16, pp. 798–836.

VICKERY, B. J. 1966 Fluctuating lift and drag on a long cylinder of square cross-section in a smooth and in a turbulent stream. *J. Fluid Mech.* **25**, 481–494.